Schizophrenia Research 204 (2019) 214–221

Contents lists available at ScienceDirect

Schizophrenia Research

journal homepage: www.elsevier.com/locate/schres

Neural correlates of reality filtering in schizophrenia spectrum disorder

Raphaël Thézé [a], Aurélie L. Manuel [a], Elena Pedrazzini [a], Fabrice Chantraine [b], Maria Cristina Patru [b], Louis Nahum [a], Adrian G. Guggisberg [a], Armin Schnider [a,*]

[a] Laboratory of Cognitive Neurorehabilitation, Division of Neurorehabilitation, Department of Clinical Neurosciences, University Hospital and University of Geneva, Geneva, Switzerland
[b] Department of Mental Health and Psychiatry, University Hospital of Geneva, Switzerland

ARTICLE INFO

Article history:
Received 27 October 2017
Received in revised form 11 May 2018
Accepted 22 July 2018
Available online 26 July 2018

Keywords:
Reality filtering
Schizophrenia
EEG
Functional connectivity
Theta frequency
Biomarker

ABSTRACT

Background: A false sense of reality is a characteristic of schizophrenia spectrum disorders (SSD). Reality confusion may also emanate from posterior orbitofrontal cortex (OFC) lesions, as evident in confabulations that patients act upon and disorientation. This confusion can be measured by repeated runs of a continuous recognition task (CRT): patients increase their false positive rate from the second run on, failing to realize that an item is not a repetition within the current run. Correct handling of these stimuli, a faculty called orbitofrontal reality filtering (ORFi), induces a distinct frontal potential at 200–300 ms, the "ORFi potential". Patients with schizophrenia have been reported to fail in this task, too. Here, we explored the electrophysiology of ORFi in SSD.
Methods: Evoked potentials, source, and connectivity analyses derived from high-density electroencephalograms of 17 patients with SSD and 15 age-matched healthy controls performing two runs of a CRT.
Results: Although the patients obtained normal performance, they did not normally express the frontal potential typical of ORFi between 200 and 300 ms. Coherence analysis demonstrated virtually absent functional connectivity in the theta band within the memory network in this period. Source analysis showed increased activity in left medial temporal and prefrontal regions in patients.
Conclusions: SSD patients appear to invoke compensatory resources to handle the challenges of reality filtering. An abnormal ORFi potential may be an early biomarker of SSD.

1. Introduction

Reality distortion in thinking occurs in multiple diseases. The prototypical disorder is schizophrenia, in which hallucinations and delusions reflect a confusion about what reality is (Cullberg, 2014; Kahn and Keefe, 2013). Self-generated thoughts may be experienced as sensory perceptions in the absence of an external stimulus, leading to hallucinations (Grossberg, 2000; Hawco et al., 2015). Reality confusion has been described as a defect in filtering or gating sensory input (Andreasen et al., 1994). Schizophrenia is associated with loss of grey matter in prefrontal, medial temporal, limbic and parietal regions, and subcortical structures (Buckley, 2005; Davatzikos et al., 2005; Gur et al., 2000; Koutsouleris et al., 2008; Pantelis et al., 2003; Patru and Reser, 2015) and aberrant functional connectivity between these regions (Liu et al., 2008; Skudlarski et al., 2010). These observations support the old idea, already proposed by Kraepelin (1919/1971), that schizophrenia reflects a disconnection syndrome (Davatzikos and Koutsouleris, 2016; Friston and Frith, 1995), associated with "noisy" information processing within networks implied in perception, working memory or attention (Andreasen et al., 1998; Uhlhaas and Singer, 2010).

Reality confusion may also result from focal brain damage involving the orbitofrontal cortex (OFC) and areas connected with it. Patients confabulate their recent experiences and plans for the future, are disoriented, and act according to their false ideas. We have called this disorder, which corresponds to the original definition of the Korsakoff syndrome (Bonhoeffer, 1901), behaviorally spontaneous confabulation (Schnider, 2008). Its underlying mechanism appears to be an inability to realize when thoughts do not relate to current reality (Nahum et al., 2012; Nahum et al., 2009; Schnider et al., 2017). The patients have a specific failure when they perform repeated runs of a continuous recognition task, each of them composed of the same picture series: they increase their false positives from the second run on, believing they have just seen a picture within the "current reality" of the ongoing run when indeed they have seen it in a previous run (Nahum et al., 2012; Schnider and Ptak, 1999; Schnider et al., 1996b, a). Healthy subjects performing this task activated the posterior medial OFC and subcortical connections as observed with $H_2^{15}0$-positron emission tomography (Schnider et al., 2000b; Treyer et al., 2003). In evoked potential studies, correct processing of these stimuli (first appearances within the second run, "distracters"), induced a frontal potential at 200–300 ms (Schnider et al., 2002). We have called this mechanism Orbitofrontal

* Corresponding author at: Service de Neurorééducation, Hôpitaux Universitaires de Genève, 26, av. de Beau-Séjour, CH-1211 Geneva 14, Switzerland.
E-mail address: armin.schnider@hcuge.ch (A. Schnider).

https://doi.org/10.1016/j.schres.2018.07.036
0920-9964/

Reality Filtering (ORFi) (Schnider, 2008, 2013). Processing of the other stimuli induced a negative potential reflecting extended neocortical activation (Bouzerda-Wahlen et al., 2015; Schnider, 2003; Wahlen et al., 2011). Schizophrenic patients having auditory hallucinations have also been reported to fail in this task: they had an increase of false positives from the second run on (Badcock et al., 2005; Waters et al., 2003), suggesting that schizophrenia may also be associated with deficient ORFi.

In the present study, patients with schizophrenia spectrum disorder (SSD) performed the continuous recognition task with two runs employed in the original event-related potential (ERP) study (Schnider et al., 2002) while high-density EEG was recorded. We hypothesized that patients with SSD have deficient ORFi, evident in an increase of false positives in the second run, and that this failure is electrophysiologically characterized by: (1) abnormality of the frontal 200–300 ms potential associated with normal processing of the "distracters" (first appearances) of the second run; (2) abnormal network interactions with reduced functional connectivity during processing of these stimuli.

2. Materials and methods

2.1. Participants

Patients were recruited at the Division of General Psychiatry at the University Hospitals of Geneva. Inclusion criterion was a diagnosis of SSD according to the International Statistical Classification of Diseases and Related Health Problems (ICD-10). Exclusion criteria were unwillingness to participate (e.g. due to fear of EEG recording), or cognitive or other difficulties in understanding task instructions as estimated by the treating psychiatrist. Of 20 patients initially recruited, one subsequently had to be excluded because of severe memory impairment interfering with comprehension of the task, two because of extreme noise in the EEG. The remaining 17 patients (4 women; 2 left handed; age 28.5 ± 9.1 years) had the following diagnoses: paranoid schizophrenia (F20.0; $N = 10$), undifferentiated schizophrenia (F20.3; $N = 3$), chronic hallucinatory psychosis (F28.0, $N = 2$), schizoaffective disorder (F25.0; $N = 1$), and unspecified psychosis (F29.0; $N = 1$). At the time of the experiment, patients received their usual medication including neuroleptics ($n = 15$ patients), antidepressants ($n = 3$), or benzodiazepines ($n = 4$). Five patients consumed cannabis.

In addition, 20 age-matched healthy paid subjects with no history of neurological or psychiatric illness partook in the study. Five were subsequently excluded: three because of a noise in the recordings, two because of technical issues during recording, leaving 15 subjects for analysis (4 women; 1 left handed; age 29.9 ± 13.1 years). Group demographics are summarized in Table 1.

All subjects gave written informed consent to participate in the study, which was approved by the Ethics Committee of the Canton of Geneva and conducted according to the Declaration of Helsinki.

Table 1
Demographics of controls and patients. Group comparisons are indicated in the right column. A chi-square test was used to test for differences between groups for sex and laterality. Other differences were tested with unpaired *t*-tests. An asterisk marks significant results with $p < 0.01$. and n.a. indicates not applicable.

Description	Patients ($n = 17$)		Controls ($n = 15$)		Comparison
	Mean	SD±	Mean	SD±	*p*-Value
Age (years)	28.5	9.1	29.9	13.1	0.73
Sex (M/W)	13/4	n.a.	11/4	n.a.	0.63
Education (years)	12.1	2.2	14.4	2.4	<0.01*
Laterality (L/R)	2/15	n.a.	1/14	n.a.	0.31
Diagnosis (years)	6.7	6.2	n.a	n.a	n.a

2.2. Psychiatric and neuropsychological testing

Psychosis was scored using the Brief Psychiatric Rating Scale (BPRS) (Ventura et al., 1993).

All participants underwent the following neuropsychological tests: Verbal learning using a 12 words test (Wechsler III, 2001), Stroop test (Bayard et al., 2009), verbal fluency (Thurstone and Thurstone, 1962), figural fluency (Regard et al., 1982), Color Trail making test (Maj et al., 1993), digit span (Wechsler, 1945) and orientation (Von Cramon and Säring, 1982).

2.3. Paradigm

Participants performed the task previously used by Schnider et al. (2002). It consists of two runs of a continuous recognition task composed of the same set of line drawings, re-arranged in different order in both runs. The pictures were colored versions (Rossion and Pourtois, 2001) of the line drawings of Snodgrass and Vanderwart (1980), presented on a 17-inch monitor, at the size of 8° of visual angle. Stimuli were presented for 1000 ms; interstimulus interval, with a fixation cross on the screen, was 2000 ms. Both runs were composed of 48 different pictures, of which 6 reappeared once and 15 reappeared twice as targets during the run. Thus, a run had 48 first appearances ("distracters") and 36 repetitions ("targets"), totaling 84 picture presentations. A run lasted about 8 min. The second run started about 1 min after the end of the first.

In both runs, subjects were required to indicate by button press (index of the right hand for "yes", middle finger for "no") whether they had already seen the presented picture "within, and only within", the ongoing run.

To obtain enough evoked responses, participants performed a second block of the same task, composed of a completely new set of pictures, which started 10 min after completion of the first block. Data of the two blocks were pooled, yielding a total of 96 distracters (first within-run presentations) and 72 targets (repetitions) for the combined first runs and a similar number for the combined second runs. In the following, Dis1 and Dis2 denote distracters of run 1 and 2; Tar1 and Tar2 denote targets (within-run repetitions) of run 1 and 2.

The critical stimuli are the distracters of the second run (Dis2), which require the feeling that the memory of a stimulus, albeit familiar from presentation in the preceding run, is currently irrelevant; the memory does not pertain to the current reality of the ongoing run (Schnider, 2003; Schnider and Ptak, 1999). Confabulating patients specifically failed on these stimuli, resulting in an increase of false positives in the second run (Nahum et al., 2012; Schnider and Ptak, 1999; Schnider et al., 1996a). Recovery from reality confusion was accompanied by a decrease (normalization) of the number of false positives in the second run (Schnider et al., 2000a).

2.4. Behavioral analysis

Demographic and neuropsychological data in the two groups were compared using unpaired Student *t*-tests. Patients' neuropsychological test scores, which significantly differed from the controls, were tested for correlation with five measures of the BPRS considered particularly relevant for reality distortion (hallucinations, unusual thoughts content, bizarre behavior, disorientation and conceptual disorganization) using Pearson's tests with Bonferroni correction.

To analyze performance in the experimental task, the percentages of correct responses and reaction times were subjected to 2 × 2 × 2 mixed model repeated measure ANOVA (rmANOVA) with Stimulus (Distracter, Target) and Run (1 or 2) as within subject factors and Group (Patient, Control) as between-subjects factor. Percentages of correct responses were further correlated with the five selected measures of the BPRS.

2.5. Data acquisition and pre-processing

Electroencephalography (EEG) recordings were conducted on the PyCorder software with a 156-channel Brain Products machine equipped with BrainVision actiCHamp amplifier and actiCAP active electrodes (*Brain Products GmbH, Germany*) at a sampling rate of 500 Hz. Pre-processing and inverse solutions were done with the Cartool software developed by Denis Brunet (https://sites.google.com/site/cartoolcommunity/home). Epochs were defined 400 ms pre-stimulus onset to 600 ms post-stimulus onset. Data were band-pass filtered (3–45 Hz). Epochs with substantial eye blinks, eye movements, muscular contractions, or electrodes artefacts were excluded by visual inspection.

Artefact-free epochs were averaged as a function of Run (1 or 2) and Stimulus (Distracter or Target) for each subject individually. Bad channels containing artefacts persistent across epochs were interpolated from neighboring electrodes using a 3D spline interpolation (<5% interpolated electrodes; (Perrin et al., 1987)) and recalculated against the average reference. ERPs were then grand-averaged between all subjects of the two groups separately with a baseline correction using the 400 ms pre-stimulus period.

2.6. Cluster waveform analysis

The main interest of this analysis was the ORFi frontal potential. We selected a frontal cluster of electrodes among 14 clusters defined in a global waveform analysis (see supplemental information) and for which all the electrodes displayed significant interaction between factors Stimulus (Distracter and Target) and Run (1 and 2). These electrodes corresponded to the Fz, F2, FFC2h, FFC4h, FCz, FC2, FC4, FCC2h and FCC4h electrodes position of the 160Ch Standard Electrode Layout for actiCHamp based on the 10/20 system. Data from these electrodes were exported to Matlab (The MathWorks Inc., Natick, USA) for further analysis.

Average amplitudes of the cluster electrodes were compared between stimuli for significant interaction over the post-stimulus onset period from 0 to 600 ms with 2 × 2 rmANOVAs with factors Stimulus (Distracter and Target) and Run (1 and 2) for both groups separately. In the case of significant interactions, paired *t*-tests were conducted.

2.6.1. Group comparison

To compare the frontal ERPs induced by our main stimulus of interest (Dis2) in the two groups, we determined the mean amplitudes in response to each stimulus in the time windows in which the two groups had a significant Stimulus (Dis, Tar) × Run (1 and 2) interaction in the cluster analysis. For each group, we then subtracted the mean amplitudes evoked by Dis1, Tar1 and Tar2 stimuli from the amplitudes evoked by Dis2 in the two groups. The ensuing relative amplitude of Dis2 was then compared between the groups with paired *t*-test.

To verify that ERP differences were not merely due to medication, we additionally performed a multivariate logistic regression including intake of psychoactive substances as binary confounding covariate for each class (antidepressants, neuroleptics, benzodiazepine and cannabis).

2.7. Source analysis

To compare activity in response to Dis2 stimuli between the two groups, we used a distributed linear inverse solution based on Local Auto-Regressive Average (LAURA) to estimate the generators of electrical potentials in both groups from 0 to 600 ms (Grave de Peralta Menendez et al., 2001; Grave de Peralta Menendez et al., 2004; Michel and Murray, 2012). The solution space is based on a 3D realistic head model comprising 4146 nodes distributed within the grey matter of the average brain provided by the Montreal Neurological Institute. The resulting local electrical current densities at each node were statistically compared between controls and patients for Dis2 stimuli with time-point wise paired t-tests using Cartool. To correct for temporal autocorrelation and multiple testing, only periods with $p < 0.05$ for at least 20 ms were retained (Guthrie and Buchwald, 1991; Manuel and Schnider, 2016; Toepel et al., 2014).

2.8. Functional connectivity

Network dynamics underlying ORFi were explored with a functional connectivity analysis performed in Matlab using the Functional Connectivity Mapping (FCM) toolbox (Guggisberg et al., 2011) in NUTMEG (Dalal et al., 2011)

http://www.nitrc.org/plugins/mwiki/index.php/nutmeg:MainPage.

Event-related coherence changes (ERCoh) during the task (Andrew and Pfurtscheller, 1996) were assessed as described previously (Thézé et al., 2016) and in the supplemental information. ERCoh was computed for each condition as the magnitude squared coherence between all grey matter voxel pairs, in each time window and through *theta* (3–7.5 Hz), *alpha* (7.5–12 Hz), *beta* (12–30 Hz) and *gamma* (30–45 Hz) frequencies. Global functional connectivity (FC) was calculated as the average ERCoh of a given voxel with all other voxels. This corresponds to the graph theoretical measure of weighted node degree and can be seen as an index of the overall importance of a brain area in the network (Newman, 2004; Stam and Van Straaten, 2012).

2.8.1. Seed analysis

ROIs with enhanced global connectivity (i.e, weighted node degree), were then selected as seed regions in order to find their main areas of interaction.

3. Results

3.1. Psychiatric and neuropsychological testing

Patients had a BPRS score of 49.25 ± 13.87 on average, corresponding to “moderately” to “markedly” severe psychosis (Leucht et al., 2005).

Table 2 summarizes neuropsychological test scores of patients and controls. Patients obtained lower scores only on categorical verbal fluency; all other measures were similar between the groups.

Correlations between the neuropsychological measure of verbal fluency and the “reality distortion” measures from the BPRS (hallucinations, unusual thoughts content, bizarre behavior, disorientation, conceptual disorganization) were not significant.

Table 2
Results from the neuropsychological evaluation of controls and patients. Group comparisons (right column) were performed with unpaired t-tests. An asterisk marks significant results with $p < 0.01$.

Description	Patients (n = 17)		Controls (n = 15)		Comparison
	Mean	SD	Mean	SD	*p*-Value
12 words (Wechsler III, 2001)					
Total immediate recall	32.6	8.3	37.1	3.7	0.055
Delayed recall	7.0	3.0	8.7	2.2	0.072
Stroop (Bayard et al., 2009)					
Errors	0.4	1.1	0.3	0.8	0.095
Time (sec)	25.9	11.1	23.2	23.2	0.53
Fluency					
Categorical	25.6	9.8	35.2	9.2	<0.01*
Phonological (Thurstone and Thurstone, 1962)	21.8	6.2	25.3	9.5	0.23
Five points (Regard et al., 1982)	29.4	7.2	33.2	8.1	0.17
Color Trail 1 (sec) (Maj et al., 1993)	36.4	18.4	34.3	13.8	0.72
Color Trail 2 (sec) (Maj et al., 1993)	86.3	44.7	75.5	49.2	0.52
Digit span (Wechsler, 1945)	9.6	2.2	10.5	2.5	0.38
Orientation (Von Cramon and Säring, 1982)	19.6	0.9	19.9	0.4	0.34

3.2. Behavioral analysis

Table 3 summarizes the behavioral results on the task. A rmANOVA on accuracy (% hits) revealed a main effect of Run and Stimulus in both groups (Run: $F_{(2,30)} = 28.5$, $p < 0.01$; Stimulus: $F_{(2,30)} = 13.6$, $p < 0.01$): subjects were more accurate on distracters and on stimuli of run1 in general, but there was no significant difference between groups. There were no "missed" stimuli, and thus accuracy is inversely related to false responses.

A rmANOVA on reaction times revealed that target stimuli were processed faster than distracters ($F_{(2,30)} = 8.1$, $p < 0.01$) in general, but there was no significant difference between the groups.

Of the five "reality distortion" measures retained from the BPRS, only unusual thought content correlated with the accuracy of Dis1 ($r = -0.53$, $p = 0.027$).

3.3. Cluster waveform analysis

Evoked potential analysis was based on a similar number of retained responses in both groups. In the patient group, the number of retained epochs was: 54 ± 17 for Dis1, 42 ± 13 for Tar1, 56 ± 16 for Dis2 and 40 ± 11 for Tar 2. In the control group, it was: 55 ± 17 for Dis1, 43 ± 13 for Tar1, 57 ± 17 for Dis2 and 41 ± 12 for Tar2. A 2 × 2 rmANOVA (Run x Stimulus) indicated no effect of group or run ($p > 0.05$). However, there were more epochs for the Distracter items than Targets (Patients: $F(1,14) = 65$, $p < 0.01$; Control: $F(1,14) = 14.5$, $p < 0.01$), which reflects the design of the experiment (96 Distracters presented in each run, 72 Targets).

Fig. 1 shows the waveform analysis on the frontal cluster.

In the control group (Fig. 1A), time-wise rmANOVA on the waveform amplitude revealed a Stimulus x Run interaction between 240 and 320 ms ($F(1,14) = 7.1$, $p = 0.018$; Fig. 1A) due to Dis2 inducing a less negative amplitude than all other stimuli. There were additional effects in the frontal cluster in the 450–550 ms time-window with a main effect of stimulus, where target stimuli were more positive than distracters ($F(1,14) = 14.9$, $p < 0.01$; Fig. 1A).

In the patient group (Fig. 1B), time-wise rmANOVA on the waveform amplitude at the same frontal cluster revealed a Stimulus x Run interaction ($F(1,16) = 7.1$, $p = 0.017$; Fig. 1B) from 270 to 300 ms. Additional main effects of Stimulus ($F(1,16) = 7.2$, $p = 0.016$) and Run ($F(1,16) = 12.2$, $p < 0.01$) were observable for the time period from 500 to 550 ms (Fig. 1B) with Tar1 being more positive and Dis2 being more negative than the other two stimuli.

3.3.1. Group comparison

Relative amplitudes of Dis2 stimuli, as described in Section 2.6.1, were compared between groups. The average waveform amplitude at the right frontal cluster was significantly more negative in the patient group between 270 and 300 ms than in the control group over 240–320 ms ($t(16) = 2.52$, $p = 0.017$).

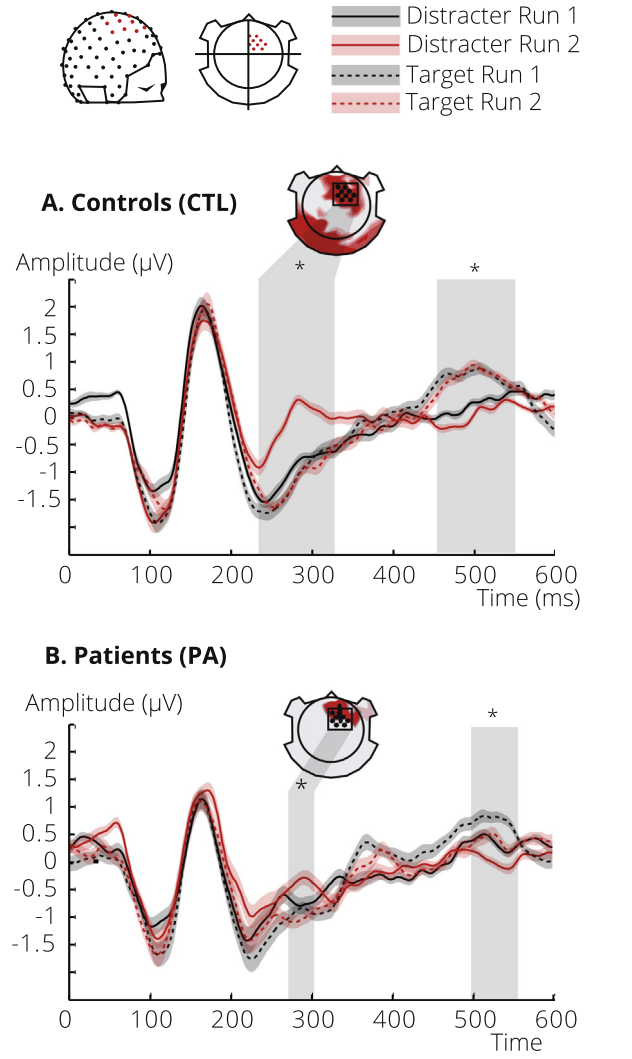

Fig. 1. Frontal cluster waveform analysis. (A) Controls, (B) patients. The extent of the frontal cluster of electrodes is represented at the top of the figure. Waveforms are reported with standard error of the mean between 0 and 600 ms for each stimulus type. Grey columns indicate periods of significant amplitude differences; the whole-scalp layout on top shows the electrical field configuration for the duration of the effect with red indicating electrodes with significant interaction effect.

Table 3
Performance in the experimental task. Average correct answers (Hits), in percentage, and reaction times (RT), in milliseconds, with standard deviation, for distracters and targets of both runs of the task and for both the control and the patient groups. The right column reports the result from the direct comparison.

	Stimuli	Hits (%)	SD	RT (ms)	SD
Patients	Dis1	98.9	1.6	1099.7	327.9
	Tar1	92.2	7.7	987.8	291.5
	Dis2	96.4	3.7	1066.8	350.4
	Tar2	88.6	9.8	988.8	222.8
Controls	Dis1	98.9	1.1	871.6	250.0
	Tar1	94.8	5.9	830.4	265.1
	Dis2	94.2	6.7	969.9	359.0
	Tar2	93.1	8.7	882.2	288.9

To verify that group differences were not just due to medication intake, we performed a multivariate logistic regression analysis with the relative ERP amplitude of Dis2 stimuli and including medication intake as binary confounding covariate for each category of substance (antidepressants, neuroleptics, benzodiazepine and cannabis). Under this condition, ERP amplitude differences remained significant (beta = −1.5, $t = -2.76$, $p = 0.01$) and independent of medication intake (beta = 0.12, $t = 2.87$, $p < 0.01$; Final model: $F(5,26) = 4.8$; $R^2 = 0.48$; $p < 0.01$).

3.4. Source analysis

Dis2 stimuli evoked stronger current density in patients than controls in diverse regions in four periods (Fig. 2): (1) right medial temporal (MTL) area at about 200–240 ms; (2) left fronto-temporal region at about 270–290 ms; (3) left MTL and left ventrolateral prefrontal cortex at about 400–430 ms; (4) right MTL at about 525–550 ms. There were also significant early differences (0–100 ms) with diffuse localization.

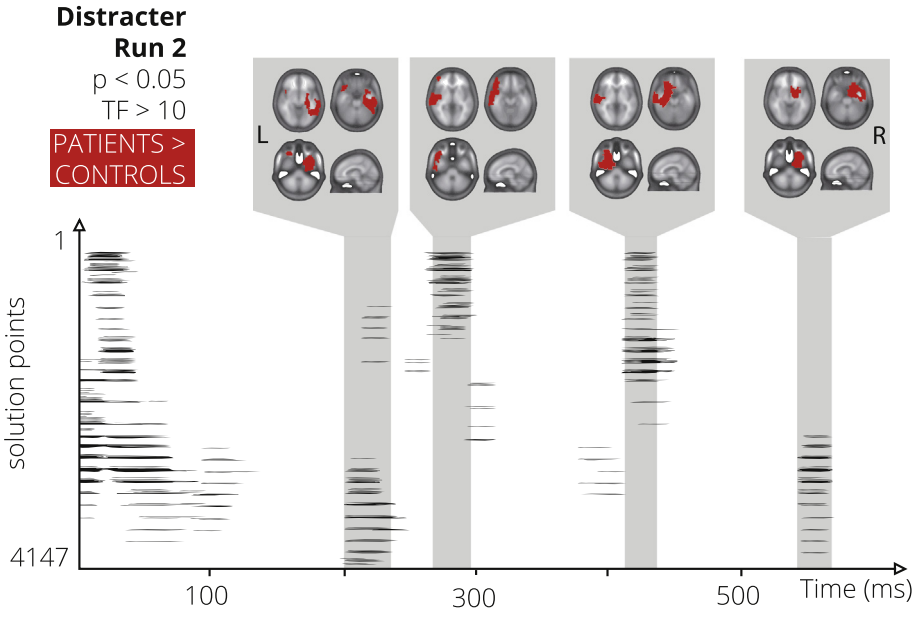

Fig. 2. Inverse solution. Unpaired comparison between controls and patients from 0 to 600 ms. Solution points in the template are represented on the y-axis. Significant effects are illustrated with black lines for time periods when $p < 0.05$ for at least >20 ms. Brain slices on top illustrate in red the corresponding brain activations. All effects were stronger in the patient group.

3.5. Functional connectivity

Fig. 3A shows that, in controls, Dis2 stimuli triggered a significant increase of coherence from baseline in the theta-band frequency between 100 and 300 ms ($p < 0.05$, cluster corrected). There was no significant coherence change in response to Dis1, Tar1, or Tar2. Regions with a significant increase of coherence were centered on the OFC, left hippocampus (LHC), anterior cingulate cortex (ACC) and left fusiform gyrus (LFG). Fig. 3B shows that the ROIs corresponding to these regions increased their global theta ERCoh from baseline specifically in response to Dis2 stimuli at 100–300 ms.

There was no significant coherence change specific for Dis2 in the alpha, beta and gamma frequencies.

The patient group displayed no significant increase of coherence in the theta frequency throughout the brain at any point in time.

Fig. 3C shows the direct comparison between the groups at 100–300 ms: Dis2 stimuli induced significantly more coherence in the theta frequency in the control group than in the patient group in OFC, LHC, ACC and LFG.

3.5.1. Seed analysis

Fig. 4 shows coherence magnitude between the four ROIs as a function of time in controls (Fig. 4A) and patients (Fig. 4B). Statistical results here refer to the average ERCoh being significantly different from baseline in response to Dis2, with $t(14) > 2.15$, $p < 0.05$ for the controls and $t(16) > 2.12$, $p < 0.05$ for the patients (Fig. 4) and are marked with an asterisk for each time window on the figure.

In the control group (Fig. 4A), the OFC had increased coherence ($t(16) > 2.12$, $p < 0.05$) with the LHC between 100 and 300 ms. The LFG had increased coherence with the OFC and LHC between about 100 and 300 ms. The ACC had increased coherence with the OFC at 100–150 ms and the LHC between 150 and 350 ms. In total there were 5 pairs of significant interactions.

In the patient group (Fig. 4B), there was no significant increase of ERCoh (all $t(14) < 2.15$, $p > 0.05$) between any of the ROIs at any time. The theta-band ERCoh between the LFG and LHC, but not the other ROIs, inversely correlated at 100–300 ms with the level of hallucinations ($r = -0.58$; $p = 0.015$ uncorrected). However, when corrected for multiple comparisons, this correlation was not significant ($p = 0.075$, Bonferroni corrected).

4. Discussion

This study used a paradigm with confirmed clinical validity for the reality confusion characterizing behaviorally spontaneous confabulation and disorientation after orbitofrontal damage or disconnection (Schnider, 2003, 2008; Schnider and Ptak, 1999). In the present study, the successful performance of the task by healthy subjects again induced a distinct frontal potential at about 200–300 ms in response to the stimuli on which reality confusing patients had failed in the clinical studies: first appearances in the second run, or "distracters" of run 2 (Dis2). This result confirms previous evoked-potential studies (Bouzerda-Wahlen et al., 2015; Schnider et al., 2002; Wahlen et al., 2011). The new finding of this study is that, subjects with SSD did not normally express this potential (the "ORFi potential") in response to the critical stimuli. Indeed, the attenuation of this potential was predictive of having SSD.

The finding complements a list of electrophysiological biomarkers of schizophrenia. The P50, an early reaction to redundant auditory stimuli is decreased in schizophrenia (Bramon et al., 2004). So are the P300 (Bramon et al., 2004; Mathalon et al., 2000; Winterer et al., 2001), a central positivity normally occurring from about 250 to 500 ms, and the Mismatch Negativity (MMN) (Kremláček et al., 2016), a bilateral posterior negativity, which – with visual stimuli – is normally expressed between 200 and 350 ms, depending on the precise stimulus parameters (MMN is more often tested in the auditory modality).

The ORFi potential reflects a cognitive process that is clearly different from the P300 and MMN, which arise in response to infrequent, unexpected stimuli. In our task, the Dis2 stimuli are familiar to the subject (from the first run) and slightly more frequent than the stimulus repetitions (targets). Of note, although the first and second run of the task have exactly the same design, only Dis2 stimuli are falsely recognized as within-run repetitions by reality confusing patients (Nahum et al., 2012; Schnider and Ptak, 1999; Schnider et al., 1996a) and only these stimuli induce the ORFi potential (Bouzerda-Wahlen et al., 2015; Schnider et al., 2002; Wahlen et al., 2011). Patients recovering from reality confusion specifically recover the ability to handle these stimuli (Schnider et al., 2000a). Being unable to process these stimuli signals a

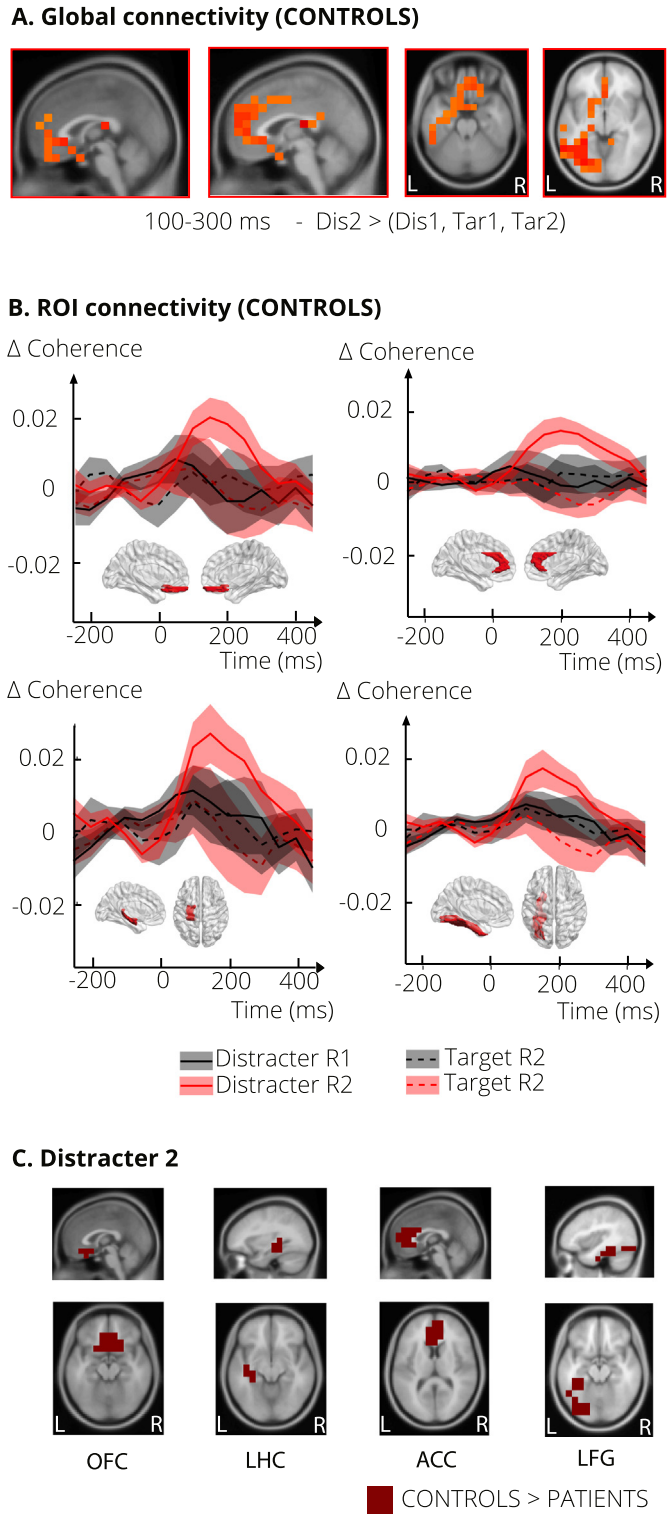

Fig. 3. Event-Related Coherence changes. In both groups the Event-Related Coherence (ERCoh) was measured for every voxel of the brain to every other voxels of the brain. (A) Voxels from the control group with significant increase of coherence ($p < 0.05$) in response to Dis2 stimuli at 100–300 ms are displayed on a template. Voxels correspond to (from left to right) anterior cingulate (2 slices), the left hippocampus and the left fusiform gyrus, and orbitofrontal cortex. (B) Coherence in these four regions, indicated as ROIs, over 600 ms. The curves indicate theta coherence fluctuations with standard error of the mean for each stimulus type. In all regions, significant theta coherence differences are limited in time (around 100–300 ms) and specific for responses to Dis2 stimuli. (C) Areas with stronger coherence in control subjects than patients in the period 100–300 ms.

failure to sense that an upcoming memory does not pertain to current reality (Schnider, 2018). Although this paradigm has been applied here only for the first time in a psychiatric population with EEG recordings, it might serve as a novel biomarker of SSD with a cognitive background closer to the nature of the disease than the P300 and MMN.

Coherence analysis provided a possible explanation for the abnormally weak ORFi potential. As healthy subjects responded to the Dis2 stimuli, their OFC, ACC, LHC and LFG specifically increased their coherence with the rest of the brain in the theta frequency (Fig. 3). These global coherence changes correspond to an increase in weighted node degree in graph theory and can be interpreted as increased importance of these areas in the brain network (Newman, 2004; Stam and Van Straaten, 2012). This occurred in the same period in which the ORFi potential was expressed (coherence analysis has much lower temporal precision than waveform analysis). In the SSD patients, this increase of theta coherence was virtually absent.

Communication between these four regions was not normal, either. As the seed analysis showed (Fig. 4), coherence between them was enhanced in the theta frequency from 100 to 300 ms in control subjects, but not in SSD patients. We may speculate that this decreased coherence was at the basis of the practically absent ORFi potential in the patients.

Coherence in the theta frequency has been related to cortico-hippocampal feedback loops implied in memory processing (Buzsáki, 2002; Miller, 2013) as well as to long distance synchronization between large neuronal assemblies (Von Stein and Sarnthein, 2000). Innumerable studies have documented grey matter reductions in frontal and temporal regions, including HC and OFC (Davatzikos et al., 2005; Gur et al., 2000; Koutsouleris et al., 2008; Zhang et al., 2015) as well as widespread alterations of white matter tracts in schizophrenic subjects (Kubicki et al., 2002; van den Heuvel et al., 2010; Wheeler and Voineskos, 2014; Zalesky et al., 2011). However, while these studies documented abnormalities under static conditions (e.g. resting state), our observations demonstrate that abnormal connectivity in SSD may surface in a task and time specific fashion – in our case in a finite period of time (around 200 ms) during the processing of a specific type of stimulus (Dis2).

The surprising result of the study was that, despite a virtually absent ORFi potential and abnormally weak coherence, our patients with SSD still succeeded in performing the task. This result is at odds with at least two studies using a similar paradigm with four runs (Badcock et al., 2005; Waters et al., 2003), similar to the one used in one of our studies (Schnider and Ptak, 1999). Schizophrenic patients having auditory hallucinations had more false positives than healthy controls and non-hallucinating patients from run 2 on (Badcock et al., 2005; Waters et al., 2003). The different results may be due to their patients being in a more active phase of the disease; patients in our study were not experiencing hallucinations at the time they performed the task. In addition, their patients had substantial cognitive disturbances, while our patient group obtained essentially normal neuropsychological results. These observations suggest that, as the disease worsens, even temporarily, patients may fail on repeated runs of a continuous recognition task, similar to behaviorally spontaneous confabulators.

Source estimation, which allows one to localize the brain activations underlying the waveforms (Michel et al., 2004), gave a hint at how SSD patients maintained normal performance despite abnormal connectivity: Processing of the critical stimuli (Dis2) by patients induced stronger activation in left prefrontal cortex and MTL regions than in healthy subjects (Fig. 2) as well as widespread very early activations. This occurred not only during the period in which healthy subjects expressed the ORFi potential (right MTL at 200–240 ms; left fronto-temporal at 270–290 ms), but also afterwards (left MTL at 400–430 ms; right MTL at 525–550 ms). In the very early phase of processing (<100 ms), SSD patients had diffuse, not clearly localized activity, possibly consistent with previously demonstrated abnormal early visual processing, e.g. in illusory contour processing (Foxe

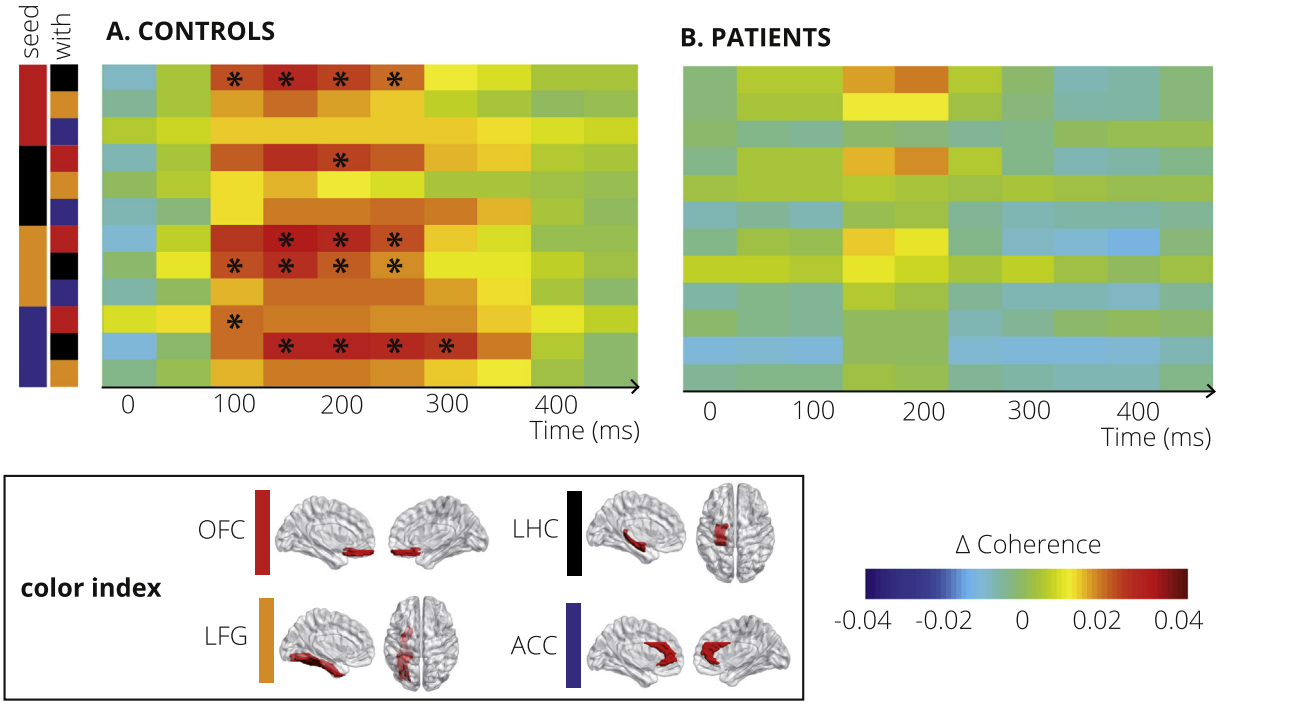

Fig. 4. Theta coherence increase between ROIs. (A) Control group, (B) SSD patients. The four ROIs are indicated along the y-axis by color-codes. The x-axis covers overlapping time windows of 300 ms every 50 ms between 0 and 600 ms (the axis stops at 450 ms because the time windows cannot overlap beyond that point). Asterisks indicate significant coherence increases from baseline.

et al., 2005). A caveat concerning these localizations is, however, that the sample size in our study was relatively small. It is possible that large groups of patients would allow one to sort out different activation patterns corresponding to precise symptomatology.

While the precise role of these relative local hyperactivities is unclear, they might indicate attempts at – obviously successful – compensation of abnormal brain function, comparable to the abnormal brain activations in patients with Alzheimer's disease performing a memory task; these activations, too, have been suggested to reflect compensation mechanisms (Desgranges et al., 1998; Erk et al., 2011; Gould et al., 2006). In schizophrenia, abnormal, presumably partly compensatory activations have previously been described during working memory (Quintana et al., 2003) and executive tasks (Minzenberg et al., 2009). From this perspective, the additional brain activations observed in our group of SSD patients might suggest increased efforts to solve the continuous recognition task. However, patients' reaction times were not significantly longer. More importantly, increased effort would neither explain the main ERP findings relating to the early period of 200–300 ms (absence of the ORFi potential, different activation in this period) nor the strikingly weaker coherence in the patient group.

In conclusion, cognitively intact subjects with SSD, who still succeed in the orbitofrontal reality filtering task, do not express the typical 200–300 ms frontal potential normally associated with the task and display defective brain connectivity in this period. It seems that SSD patients have to invoke more neural resources than healthy controls to maintain performance, possibly indicating a compensation strategy. The evoked potential response to the challenges of ORFi may be a useful, cognitively defined biomarker for SSD.

Conflict of interest

The authors declare no conflict of interest.

Role of funding source

http://www.snf.ch/en/theSNSF/profile/mission-statement/Pages/default.aspx

Acknowledgment

Supported by the Swiss National Science Foundation, grant no. 32003B_155947/1 to AS. The authors declare no competing financial interest.

Appendix A. Supplementary data

Supplementary data to this article can be found online at https://doi.org/10.1016/j.schres.2018.07.036.

References

Andreasen, N.C., Arndt, S., Swayze, V., Cizadlo, T., Flaum, M., O'Leary, D., Ehrhardt, J.C., Yuh, W.T., 1994. Thalamic abnormalities in schizophrenia visualized through magnetic resonance image averaging. Science 266 (5183), 294–298.

Andreasen, N.C., Paradiso, S., O'leary, D.S., 1998. "Cognitive dysmetria" as an integrative theory of schizophrenia: a dysfunction in cortical-subcortical-cerebellar circuitry? Schizophr. Bull. 24 (2), 203–218.

Andrew, C., Pfurtscheller, G., 1996. Event-related coherence as a tool for studying dynamic interaction of brain regions. Electroencephalogr. Clin. Neurophysiol. 98 (2), 144–148.

Badcock, J.C., Waters, F.A., Maybery, M.T., Michie, P.T., 2005. Auditory hallucinations: failure to inhibit irrelevant memories. Cogn. Neuropsychiatry 10 (2), 125–136.

Bayard, S., Erkes, J., Moroni, C., 2009. Test du Stroop Victoria-Adaptation Francophone. CPCN-LR, Gignac.

Bonhoeffer, K., 1901. Die akuten Geisteskrankheiten der Gewohnheitstrinker: eine klinische Studie. Fischer.

Bouzerda-Wahlen, A., Nahum, L., Liverani, M.C., Guggisberg, A.G., Schnider, A., 2015. An electrophysiological dissociation between orbitofrontal reality filtering and context source monitoring. J. Cogn. Neurosci. 27 (1), 164–174.

Bramon, E., Rabe-Hesketh, S., Sham, P., Murray, R.M., Frangou, S., 2004. Meta-analysis of the P300 and P50 waveforms in schizophrenia. Schizophr. Res. 70 (2), 315–329.

Buckley, P.F., 2005. Neuroimaging of schizophrenia: structural abnormalities and pathophysiological implications. Neuropsychiatr. Dis. Treat. 1 (3), 193.

Buzsáki, G., 2002. Theta oscillations in the hippocampus. Neuron 33 (3), 325–340.

Cullberg, J., 2014. Psychoses: An Integrative Perspective. Routledge, London.

Dalal, S.S., Zumer, J.M., Guggisberg, A.G., Trumpis, M., Wong, D.D., Sekihara, K., Nagarajan, S.S., 2011. MEG/EEG source reconstruction, statistical evaluation, and visualization with NUTMEG. Comput. Intell. Neurosci. 2011, 758973.

Davatzikos, C., Koutsouleris, N., 2016. Chapter 15 - Computational Neuroanatomy of Schizophrenia, the Neurobiology of Schizophrenia. Academic Press, San Diego, pp. 263–282.

Davatzikos, C., Shen, D., Gur, R.C., Wu, X., Liu, D., Fan, Y., Hughett, P., Turetsky, B.I., Gur, R.E., 2005. Whole-brain morphometric study of schizophrenia revealing a spatially complex set of focal abnormalities. Arch. Gen. Psychiatry 62 (11), 1218–1227.

van den Heuvel, M.P., Mandl, R.C., Stam, C.J., Kahn, R.S., Pol, H.E.H., 2010. Aberrant frontal and temporal complex network structure in schizophrenia: a graph theoretical analysis. J. Neurosci. 30 (47), 15915–15926.
Desgranges, B., Baron, J.-C., de la Sayette, V., Petit-Taboué, M.-C., Benali, K., Landeau, B., Lechevalier, B., Eustache, F., 1998. The neural substrates of memory systems impairment in Alzheimer's disease. A PET study of resting brain glucose utilization. Brain 121 (4), 611–631.
Erk, S., Spottke, A., Meisen, A., Wagner, M., Walter, H., Jessen, F., 2011. Evidence of neuronal compensation during episodic memory in subjective memory impairment. Arch. Gen. Psychiatry 68 (8), 845–852.
Foxe, J.J., Murray, M.M., Javitt, D.C., 2005. Filling-in in schizophrenia: a high-density electrical mapping and source-analysis investigation of illusory contour processing. Cereb. Cortex 15 (12), 1914–1927.
Friston, K.J., Frith, C.D., 1995. Schizophrenia: a disconnection syndrome. Clin. Neurosci. 3 (2), 89–97.
Gould, R., Arroyo, B., Brown, R., Owen, A., Bullmore, E., Howard, R., 2006. Brain mechanisms of successful compensation during learning in Alzheimer disease. Neurology 67 (6), 1011–1017.
Grave de Peralta Menendez, R., Gonzalez Andino, S., Lantz, G., Michel, C.M., Landis, T., 2001. Noninvasive localization of electromagnetic epileptic activity. I. Method descriptions and simulations. Brain Topogr. 14 (2), 131–137.
Grave de Peralta Menendez, R., Murray, M.M., Michel, C.M., Martuzzi, R., Gonzalez Andino, S.L., 2004. Electrical neuroimaging based on biophysical constraints. NeuroImage 21 (2), 527–539.
Grossberg, S., 2000. How hallucinations may arise from brain mechanisms of learning, attention, and volition. JINS 6 (05), 583–592.
Guggisberg, A.G., Dalal, S.S., Zumer, J.M., Wong, D.D., Dubovik, S., Michel, C.M., Schnider, A., 2011. Localization of cortico-peripheral coherence with electroencephalography. NeuroImage 57 (4), 1348–1357.
Gur, R.E., Cowell, P.E., Latshaw, A., Turetsky, B.I., Grossman, R.I., Arnold, S.E., Bilker, W.B., Gur, R.C., 2000. Reduced dorsal and orbital prefrontal gray matter volumes in schizophrenia. Arch. Gen. Psychiatry 57 (8), 761–768.
Guthrie, D., Buchwald, J.S., 1991. Significance testing of difference potentials. Psychophysiology 28 (2), 240–244.
Hawco, C., Buchy, L., Bodnar, M., Izadi, S., Dell'Elce, J., Messina, K., Joober, R., Malla, A., Lepage, M., 2015. Source retrieval is not properly differentiated from object retrieval in early schizophrenia: an fMRI study using virtual reality. NeuroImage 7, 336–346.
Kahn, R.S., Keefe, R.S., 2013. Schizophrenia is a cognitive illness: time for a change in focus. JAMA Psychiat. 70 (10), 1107–1112.
Koutsouleris, N., Gaser, C., Jäger, M., Bottlender, R., Frodl, T., Holzinger, S., Schmitt, G.J., Zetzsche, T., Burgermeister, B., Scheuerecker, J., 2008. Structural correlates of psychopathological symptom dimensions in schizophrenia: a voxel-based morphometric study. NeuroImage 39 (4), 1600–1612.
Kraepelin, E., 1919/1971. Dementia praecox. Translated by R.M. Barclay, edited by G.M. Robertson. Krieger Publishing Company.
Kremláček, J., Kreegipuu, K., Tales, A., Astikainen, P., Põldver, N., Näätänen, R., Stefanics, G., 2016. Visual mismatch negativity (vMMN): a review and meta-analysis of studies in psychiatric and neurological disorders. Cortex 80, 76–112.
Kubicki, M., Westin, C.-F., Maier, S.E., Frumin, M., Nestor, P.G., Salisbury, D.F., Kikinis, R., Jolesz, F.A., McCarley, R.W., Shenton, M.E., 2002. Uncinate fasciculus findings in schizophrenia: a magnetic resonance diffusion tensor imaging study. Am. J. Psychiatry 159 (5), 813–820.
Leucht, S., Kane, J.M., Kissling, W., Hamann, J., Etschel, E., Engel, R., 2005. Clinical implications of brief psychiatric rating scale scores. Br. J. Psychiatry 187 (4), 366–371.
Liu, Y., Liang, M., Zhou, Y., He, Y., Hao, Y., Song, M., Yu, C., Liu, H., Liu, Z., Jiang, T., 2008. Disrupted small-world networks in schizophrenia. Brain 131 (4), 945–961.
Maj, M., D'Elia, L., Satz, P., Janssen, R., Zaudig, M., Uchiyama, C., Starace, F., Galderisi, S., Chervinsky, A., 1993. Evaluation of two new neuropsychological tests designed to minimize cultural bias in the assessment of HIV-1 seropositive persons: a WHO study. Arch. Clin. Neuropsychol. 8 (2), 123–135.
Manuel, A.L., Schnider, A., 2016. Differential processing of immediately repeated verbal and non-verbal stimuli: an evoked-potential study. Eur. J. Neurosci. 43 (1), 89–97.
Mathalon, D.H., Ford, J.M., Pfefferbaum, A., 2000. Trait and state aspects of P300 amplitude reduction in schizophrenia: a retrospective longitudinal study. Biol. Psychiatry 47 (5), 434–449.
Michel, C.M., Murray, M.M., 2012. Towards the utilization of EEG as a brain imaging tool. NeuroImage 61 (2), 371–385.
Michel, C.M., Murray, M.M., Lantz, G., Gonzalez, S., Spinelli, L., de Peralta, R.G., 2004. EEG source imaging. Clin. Neurophysiol. 115 (10), 2195–2222.
Miller, R., 2013. Cortico-hippocampal Interplay and the Representation of Contexts in the Brain. Springer Science & Business Media.
Minzenberg, M.J., Laird, A.R., Thelen, S., Carter, C.S., Glahn, D.C., 2009. Meta-analysis of 41 functional neuroimaging studies of executive function in schizophrenia. Arch. Gen. Psychiatry 66 (8), 811–822.
Nahum, L., Ptak, R., Leemann, B., Schnider, A., 2009. Disorientation, confabulation, and extinction capacity: clues on how the brain creates reality. Biol. Psychiatry 65 (11), 966–972.
Nahum, L., Bouzerda-Wahlen, A., Guggisberg, A., Ptak, R., Schnider, A., 2012. Forms of confabulation: dissociations and associations. Neuropsychologia 50 (10), 2524–2534.
Newman, M.E., 2004. Analysis of weighted networks. Phys. Rev. E 70 (5), 056131.
Pantelis, C., Velakoulis, D., McGorry, P.D., Wood, S.J., Suckling, J., Phillips, L.J., Yung, A.R., Bullmore, E.T., Brewer, W., Soulsby, B., 2003. Neuroanatomical abnormalities before and after onset of psychosis: a cross-sectional and longitudinal MRI comparison. Lancet 361 (9354), 281–288.
Patru, M.C., Reser, D.H., 2015. A new perspective on delusional states–evidence for claustrum involvement. Front. Psych. 6.
Perrin, F., Bertrand, O., Pernier, J., 1987. Scalp current density mapping: value and estimation from potential data. IEEE Trans. Biomed. Eng. 4, 283–288.
Quintana, J., Wong, T., Ortiz-Portillo, E., Kovalik, E., Davidson, T., Marder, S.R., Mazziotta, J.C., 2003. Prefrontal–posterior parietal networks in schizophrenia: primary dysfunctions and secondary compensations. Biol. Psychiatry 53 (1), 12–24.
Regard, M., Strauss, E., Knapp, P., 1982. Children's production on verbal and non-verbal fluency tasks. Percept. Mot. Skills 55 (3), 839–844.
Rossion, B., Pourtois, G., 2001. Revisiting Snodgrass and Vanderwart's object database: color and texture improve object recognition. J. Vis. 1 (3) (413-413).
Schnider, A., 2003. Spontaneous confabulation and the adaptation of thought to ongoing reality. Nat. Rev. Neurosci. 4 (8), 662–671.
Schnider, A., 2008. The Confabulating Mind: How the Brain Creates Reality. first ed. Oxford University Press, Oxford.
Schnider, A., 2013. Orbitofrontal reality filtering. Front. Behav. Neurosci. 7, 67.
Schnider, A., 2018. The Confabulating Mind: How the Brain Creates Reality. second ed. Oxford University Press, Oxford.
Schnider, A., Ptak, R., 1999. Spontaneous confabulators fail to suppress currently irrelevant memory traces. Nat. Neurosci. 2 (7), 677–681.
Schnider, A., von Däniken, C., Gutbrod, K., 1996a. The mechanisms of spontaneous and provoked confabulations. Brain 119, 1365–1375.
Schnider, A., von Däniken, C., Gutbrod, K., 1996b. Disorientation in amnesia. A confusion of memory traces. Brain 119, 1627–1632.
Schnider, A., Ptak, R., von Däniken, C., Remonda, L., 2000a. Recovery from spontaneous confabulations parallels recovery of temporal confusion in memory. Neurology 55, 74–83.
Schnider, A., Treyer, V., Buck, A., 2000b. Selection of currently relevant memories by the human posterior medial orbitofrontal cortex. J. Neurosci. 20 (15), 5880–5884.
Schnider, A., Valenza, N., Morand, S., Michel, C.M., 2002. Early cortical distinction between memories that pertain to ongoing reality and memories that don't. Cereb. Cortex 12 (1), 54–61.
Schnider, A., Nahum, L., Ptak, R., 2017. What does extinction have to do with confabulation? Cortex 87, 5–15.
Skudlarski, P., Jagannathan, K., Anderson, K., Stevens, M.C., Calhoun, V.D., Skudlarska, B.A., Pearlson, G., 2010. Brain connectivity is not only lower but different in schizophrenia: a combined anatomical and functional approach. Biol. Psychiatry 68 (1), 61–69.
Snodgrass, J.G., Vanderwart, M., 1980. A standardized set of 260 pictures: norms for name agreement, image agreement, familiarity, and visual complexity. J. Exp. Psychol. Hum. Learn. Mem. 6 (2), 174–215.
Stam, C.v., Van Straaten, E., 2012. The organization of physiological brain networks. Clin. Neurophysiol. 123 (6), 1067–1087.
Thézé, R., Guggisberg, A., Nahum, L., Schnider, A., 2016. Rapid memory stabilization by transient theta coherence in the human medial temporal lobe. Hippocampus 26 (4), 445.
Thurstone, T.G., Thurstone, L.L., 1962. Primary Mental Abilities Tests. Science Research Associates.
Toepel, U., Ohla, K., Hudry, J., le Coutre, J., Murray, M.M., 2014. Verbal labels selectively bias brain responses to high-energy foods. NeuroImage 87, 154–163.
Treyer, V., Buck, A., Schnider, A., 2003. Subcortical loop activation during selection of currently relevant memories. J. Cogn. Neurosci. 15, 610–618.
Uhlhaas, P.J., Singer, W., 2010. Abnormal neural oscillations and synchrony in schizophrenia. Nat. Rev. Neurosci. 11 (2), 100–113.
Ventura, J., Green, M.F., Shaner, A., Liberman, R.P., 1993. Training and quality assurance with the brief psychiatric rating scale: "the drift busters". Int. J. Methods Psychiatr. Res. 3, 221–224.
Von Cramon, D., Säring, W., 1982. Störung der Orientierung beim hirnorganischen Psychosyndrom, Hirnorganische Psychosyndrome im Alter. Springer, pp. 38–50.
Von Stein, A., Sarnthein, J., 2000. Different frequencies for different scales of cortical integration: from local gamma to long range alpha/theta synchronization. Int. J. Psychophysiol. 38 (3), 301–313.
Wahlen, A., Nahum, L., Gabriel, D., Schnider, A., 2011. Fake or fantasy: rapid dissociation between strategic content monitoring and reality filtering in human memory. Cereb. Cortex 21 (11), 2589–2598.
Waters, F.A., Badcock, J.C., Maybery, M.T., Michie, P.T., 2003. Inhibition in schizophrenia: association with auditory hallucinations. Schizophr. Res. 62 (3), 275–280.
Wechsler, D., 1945. A standardized memory scale for clinical use. Aust. J. Psychol. 19 (1), 87–95.
Wechsler III, D., 2001. MEM-III. Échelle clinique de mémoire de Wechsler: manuel. les Éd. du Centre de psychologie appliquée.
Wheeler, A.L., Voineskos, A.N., 2014. A review of structural neuroimaging in schizophrenia: from connectivity to connectomics. Front. Hum. Neurosci. 8, 653.
Winterer, G., Mulert, C., Mientus, S., Gallinat, J., Schlattmann, P., Dorn, H., Herrmann, W., 2001. P300 and LORETA: comparison of normal subjects and schizophrenic patients. Brain Topogr. 13 (4), 299–313.
Zalesky, A., Fornito, A., Seal, M.L., Cocchi, L., Westin, C.-F., Bullmore, E.T., Egan, G.F., Pantelis, C., 2011. Disrupted axonal fiber connectivity in schizophrenia. Biol. Psychiatry 69 (1), 80–89.
Zhang, W., Deng, W., Yao, L., Xiao, Y., Li, F., Liu, J., Sweeney, J.A., Lui, S., Gong, Q., 2015. Brain structural abnormalities in a group of never-medicated patients with long-term schizophrenia. Am. J. Psychiatry 172 (10), 995–1003.